



DIGITAL ACCESS TO SCHOLARSHIP AT HARVARD

Deactivation of Akt by a Small Molecule Inhibitor Targeting Pleckstrin Homology Domain and Facilitating Akt Ubiquitination

The Harvard community has made this article openly available.

[Please share](#) how this access benefits you. Your story matters.

Citation	Jo, Hakryul, Pang-Kuo Lo, Yitang Li, Fabien Loison, Sarah Green, Jake Wang, Leslie E. Silberstein, Keqiang Ye, Hexin Chen, and Hongbo R. Luo. 2011. "Deactivation of Akt by a Small Molecule Inhibitor Targeting Pleckstrin Homology Domain and Facilitating Akt Ubiquitination." <i>Proceedings of the National Academy of Sciences</i> 108 (16) (April 4): 6486–6491. doi:10.1073/pnas.1019062108. http://dx.doi.org/10.1073/pnas.1019062108 .
Published Version	doi:10.1073/pnas.1019062108
Accessed	February 17, 2015 1:55:05 AM EST
Citable Link	http://nrs.harvard.edu/urn-3:HUL.InstRepos:13320255
Terms of Use	This article was downloaded from Harvard University's DASH repository, and is made available under the terms and conditions applicable to Other Posted Material, as set forth at http://nrs.harvard.edu/urn-3:HUL.InstRepos:dash.current.terms-of-use#LAA

(Article begins on next page)

Deactivation of Akt by a small molecule inhibitor targeting pleckstrin homology domain and facilitating Akt ubiquitination

Hakryul Jo^a, Pang-Kuo Lo^b, Yitang Li^a, Fabien Loison^a, Sarah Green^a, Jake Wang^a, Leslie E. Silberstein^a, Keqiang Ye^c, Hexin Chen^{b,1}, and Hongbo R. Luo^{a,1}

^aDepartment of Pathology, Harvard Medical School, Dana–Farber/Harvard Cancer Center, Boston, MA 02115; ^bDepartment of Biological Sciences, University of South Carolina, Columbia, SC 29208; and ^cDepartment of Pathology and Laboratory Medicine, Emory University, Atlanta, GA 30322

Edited* by Solomon H. Snyder, Johns Hopkins University School of Medicine, Baltimore, MD, and approved March 11, 2011 (received for review December 18, 2010)

The phosphatidylinositol-3,4,5-triphosphate (PIP3) binding function of pleckstrin homology (PH) domain is essential for the activation of oncogenic Akt/PKB kinase. Following the PIP3-mediated activation at the membrane, the activated Akt is subjected to other regulatory events, including ubiquitination-mediated deactivation. Here, by identifying and characterizing an allosteric inhibitor, SC66, we show that the facilitated ubiquitination effectively terminates Akt signaling. Mechanistically, SC66 manifests a dual inhibitory activity that directly interferes with the PH domain binding to PIP3 and facilitates Akt ubiquitination. A known PH domain-dependent allosteric inhibitor, which stabilizes Akt, prevents the SC66-induced Akt ubiquitination. A cancer-relevant Akt1 (e17k) mutant is unstable, making it intrinsically sensitive to functional inhibition by SC66 in cellular contexts in which the PI3K inhibition has little inhibitory effect. As a result of its dual inhibitory activity, SC66 manifests a more effective growth suppression of transformed cells that contain a high level of Akt signaling, compared with other inhibitors of PIP3/Akt pathway. Finally, we show the anticancer activity of SC66 by using a soft agar assay as well as a mouse xenograft tumor model. In conclusion, in this study, we not only identify a dual-function Akt inhibitor, but also demonstrate that Akt ubiquitination could be chemically exploited to effectively facilitate its deactivation, thus identifying an avenue for pharmacological intervention in Akt signaling.

chemical screening | cell death

A number of pathogenic conditions, including cancer, arise from perturbation of intracellular signaling pathways that control the amount of phosphatidylinositol-3,4,5-triphosphate (PIP3) at the membrane. PIP3 level is mainly controlled positively by PI3K and negatively by lipid phosphatase PTEN (1, 2). PIP3 exerts its functions by mediating the recruitment of various signaling effectors at the membrane. The serine/threonine protein kinase Akt (also known as PKB) is one of the major downstream effectors recruited by PIP3. Akt contains an N-terminal pleckstrin homology (PH) domain, which specifically binds to PIP3, enabling its membrane translocation and subsequent activation by upstream kinases (3,4). The activated Akt, in turn, phosphorylates a variety of proteins involved in diverse cellular processes, including cell proliferation and survival (5).

Because of its crucial involvement in tumorigenesis and drug resistance of cancer cells, the PIP3/Akt pathway has been the primary target for anticancer drug development (5, 6). Various current efforts to inhibit Akt function are mainly focused in two aspects: reducing PIP3 level and inhibiting Akt activity (7–11). We also showed that two inositol phosphates, InsP7 and Ins (1,3,4,5)P4, compete with PIP3 for binding to Akt PH domain (12, 13). Additionally, recent studies revealed that the ubiquitination of Akt plays important regulatory functions (14–16), providing a potential new avenue for pharmacological intervention. In this study, we identified and characterized a dual-function Akt inhibitor that directly facilitates Akt ubiquitination and deactivation. We demonstrated its efficacy toward a cancer-relevant

and PI3K inhibitor-resistant Akt1 (e17k) mutant. As a result of its dual inhibitory activity, SC66 manifests a more effective growth suppression of transformed cells compared with other inhibitors of PIP3/Akt pathway. Therefore, this study offers validation for the chemical-assisted ubiquitination as a legitimate strategy to terminate Akt signaling.

Results

Cell-Based Screening Identifies a Compound that Directly Facilitates Akt Ubiquitination. To better understand the regulatory mechanisms of the PIP3/Akt pathway, we carried out an image-based chemical screening by using the spatial distribution of Akt1 PH domain/EGFP fusion protein (PH-EGFP) as a read-out (to be described elsewhere). This screening identified a group of 12 chemicals (termed group II) that not only prevented the membrane translocation of PH-EGFP, but also induced its accumulation into a subcellular location reminiscent to the pericentrosomal region (Fig. S1 and Dataset S1). Interestingly, the compounds SC13, SC66, and SC67 contain a pyridine moiety that is also found in some chemicals known to inhibit Akt (17, 18). In this study, we focused on characterizing SC66 as a representative of this group of compounds. First, we confirmed that this subcellular location indeed represented the pericentrosomal region by immunostaining with γ -tubulin, a centrosomal marker (Fig. 1A). The SC66-induced pericentrosomal accumulation was specifically mediated by Akt PH domain, as EGFP alone or EGFP fused to PH domain from PLC- δ had no effect (Fig. 1A). Other group II compounds also showed no effect on the membrane localization of PH-PLC δ -EGFP (Fig. S2). The level of PIP3 at the membrane did not affect the SC66-induced pericentrosomal localization, as cotreatment with IGF1 or PI3K inhibitor failed to yield any differential effects. Likewise, a PIP3-nonbinding mutant PH (r25c)-EGFP was also accumulated in the pericentrosomal region. As revealed by colocalization with PH-EGFP, the full-length Akt1 could be also accumulated in this region by SC66 and other group II compounds (Fig. 1A and Fig. S3). To test if SC66 could inhibit the Akt signaling pathway, HEK293T cells, which were shown to contain a high level of PIP3 (19), were treated with different amounts of SC66, and the whole-cell lysates were examined for the phosphorylation level of Akt and its known target proteins (Fig. 1B). At a concentration that led to the pericentrosomal accumulation, SC66 significantly reduced the phosphorylation level of both Akt and its targets, but not those of other cellular kinases. Importantly, unlike the Akt phosphorylation at S473, the phosphoryla-

Author contributions: H.J., H.C., and H.R.L. designed research; H.J., P.-K.L., Y.L., F.L., S.G., and J.W. performed research; L.E.S., K.Y., and H.C. contributed new reagents/analytical tools; H.J., H.C., and H.R.L. analyzed data; and H.J., H.C., and H.R.L. wrote the paper.

The authors declare no conflict of interest.

*This Direct Submission article had a prearranged editor.

¹To whom correspondence may be addressed. E-mail: hongbo.luo@childrens.harvard.edu or hchen@biol.sc.edu.

This article contains supporting information online at www.pnas.org/lookup/suppl/doi:10.1073/pnas.1019062108/-DCSupplemental.

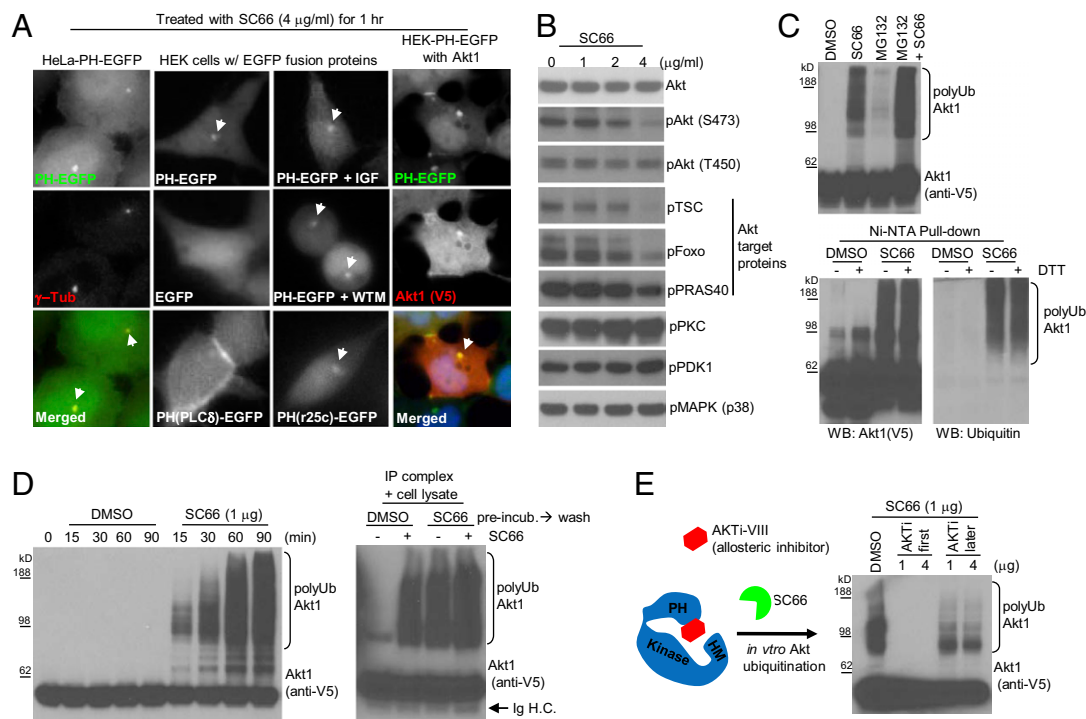


Fig. 1. Cell-based screening identifies a compound that directly facilitates Akt ubiquitination. (A) HeLa-PH-EGFP cells were treated with SC66 (4 $\mu\text{g/ml}$) for 1 h and were stained with the γ -tubulin antibody (red). Arrows indicate the colocalization of PH-EGFP with γ -tubulin (Left). HEK293 cells transfected with the indicated EGFP fusion proteins were treated with SC66 alone or together with IGF1 (20 ng/ml) or wortmannin (200 nM). After 1 h, pericentrosomal localization was visualized in live cells. Arrows indicate the pericentrosomal region (Middle). HEK293 cells stably expressing PH-EGFP were transfected with the C-terminal V5/His tagged Akt1. Following treatment with SC66 for 1 h, the fixed cells were stained for Akt1. Colocalization with PH-EGFP in pericentrosomal region is indicated by arrows (Right). (B) HEK293T cells grown in serum-rich medium were treated with different amounts of SC66 for 1 h. The whole-cell lysates were analyzed with the indicated antibodies. (C) HEK293-Akt1 cells were treated with SC66 (4 $\mu\text{g/ml}$), MG132 (10 $\mu\text{g/ml}$), or a combination of the two for 4 h, and the whole-cell lysates were analyzed by a monoclonal V5 antibody (Upper). The cell lysates from SC66-treated cells were supplemented with 50 mM imidazole followed by incubation with Ni-NTA beads in the presence or absence of 1 mM DTT. The bead-bound fraction was resolved on a SDS/PAGE and blotted with the V5 antibody for Akt1. The same membrane was autoclaved and sequentially blotted with a rabbit polyclonal antibody against ubiquitin (Lower). (D) HEK293 cell lysates were subjected to in vitro ubiquitination assay with or without SC66 for different times (Left). The Akt1 immune complex was treated with DMSO or SC66 for 1 h, and washed three times with the buffer. The resulting immune complex was subjected to in vitro ubiquitination with fresh HEK cell lysates (Right). (E) Inhibitory effect of an allosteric Akt inhibitor, AKTi-VIII, on the SC66-induced in vitro ubiquitination of Akt1.

tion at T450 was not affected by SC66, indicating that SC66 did not manifest inhibitory effects toward upstream kinase mTORc2, which was reported to be responsible for the phosphorylation of both T450 and S473 of Akt. We also tested the inhibitory effects of SC66 and other group II compounds on the Akt activation stimulated by IGF1 in HeLa cells (Fig. S4A). Overall, all these chemicals inhibited Akt phosphorylation at or below the concentration of 8 $\mu\text{g/ml}$, which is equivalent to 1 \times concentration of the initial high-throughput chemical screening. The cytoplasm to nuclear translocation of proapoptotic transcription factor Foxo1 is tightly regulated by Akt activity. To assess the effects of group II compounds on Akt function at the cellular level, we used live cell imaging by using EGFP-Foxo as a read-out (20). The majority of group II compounds were found to inhibit the cytoplasmic retention of EGFP-Foxo, whereas SC67, 86, and E26 displayed relatively weaker inhibitory activity (Fig. S4B). To determine if the group II compounds could also affect the levels of PIP3, the selected compounds were treated to serum-starved HeLa cells. Following IGF1 stimulation, the level of PIP3 was measured (Fig. S4C). Unlike the PI3K inhibitor LY294002, none of the tested group II compounds significantly reduced the PIP3 level, indicating that their inhibitory effect on the Akt phosphorylation was not caused by reduction of PIP3 level. This finding was also consistent with their inhibitory patterns of target phosphorylation, more similar to Akt inhibition than PI3K inhibition (Fig. S4A). Next, we sought to determine the mechanisms of group II-mediated inhibition of Akt activation. As these compounds did not affect the cellular PIP3 level, we explored the possibility that they may directly

interfere with the PIP3 binding function of PH domain. To test this idea, purified PH-EGFP was incubated with PIP3-coated beads in the presence of group II compounds. The amount of PH-EGFP brought down by the PIP3-beads would be inversely correlated with the inhibitory activity of compound toward the PIP3 binding function of PH domain (Fig. S4D). This assay implicated that all group II compounds, in varying degrees, could interfere with PH domain binding to PIP3 in vitro.

One of the important functions of the pericentrosomal region is the recycling and degradation of cellular proteins (21). The accumulation of Akt in this region may reflect its degradation through the ubiquitin-mediated proteasomal pathway. Indeed, when HEK293 cells stably expressing Akt1, HEK293-Akt1, were treated with SC66, a robust accumulation of the ubiquitinated Akt was observed (Fig. 1C). The level of SC66-induced Akt ubiquitination was further increased by cotreatment with the proteasome inhibitor MG132. A similar result was also observed with the endogenous Akt in HeLa cells (Fig. S5A). A longer treatment of SC66 decreased the level of total Akt in both HeLa and HEK293T cells (Fig. S5B). Together, these results confirmed that the ubiquitinated Akt by SC66 could be targeted for proteasome-mediated degradation. Some group II compounds also led to the accumulation of ubiquitinated Akt (Fig. S5C). Of note is the finding that SC67, which is structurally similar to SC66 (Fig. S1), led to a much weaker accumulation of ubiquitinated Akt. All group II compounds, including SC66, did not display any significant inhibitory effects toward the cellular proteasome or deconjugation (i.e., deubiquitination) activity

(Fig. S5D). Next, we established a cell-free system to examine if group II compounds could directly affect Akt ubiquitination (Fig. S6A). The *in vitro* ubiquitination of Akt using the control HEK293 cell extracts appeared inefficient, and only a weak level of ubiquitinated Akt could be observed. Strikingly, however, in the presence of SC66 in this cell-free system, a robust ubiquitination was observed (Fig. 1D). The enhanced *in vitro* ubiquitination of Akt by SC66 was both time- and dose-dependent (Fig. 1D and Fig. S6B). Compared with the other group II compounds in the same *in vitro* assay, SC66 displayed the strongest activity, followed by SC67 and SC11 (Fig. S6C).

To further test if the drug-bound Akt was susceptible for ubiquitination, the Akt immune complex was incubated with SC66. After removal of the compound by extensive washing, the resulting immune complex was subject to *in vitro* ubiquitination in the presence of fresh cell lysates (Fig. 1D). Intriguingly, the pretreatment of drug alone was found to be sufficient, indicating that the drug-bound Akt was amenable (or primed) for the subsequent ubiquitination.

The efficiency of ubiquitination could be dependent upon the conformation(s) of target protein. To test if this is the case for the SC66-induced Akt ubiquitination, we took advantage of a known PH domain-dependent allosteric Akt inhibitor, AKTi-VIII (22), and asked if the SC66-induced Akt ubiquitination could be affected by this inhibitor. Surprisingly, when the lysates were preincubated with AKTi-VIII, the subsequent ubiquitination by SC66 was almost completely abolished (Fig. 1E). When SC66 was added first, followed by AKTi-VIII, Akt ubiquitination was also affected, but to a lesser extent. Other chemicals known to inhibit Akt functions failed to show any inhibitory effects (Fig. S6D). Together, these results confirm that SC66 directly facilitates Akt ubiquitination.

SC66 Functionally Inhibits a Cancer-Relevant Akt1 (e17k) Mutant. A gain-of-function mutation in PH domain (e17k) of Akt1 has been identified from human cancers (23). Next, we examined if SC66 could be effective in functional inhibition of this mutant Akt1. As previously reported, when expressed in HEK293 cells, compared

with the WT, the level of phosphorylated Akt was much higher in Akt1 (e17k), and a strong enrichment of phosphorylated Akt was found at the plasma membrane (Fig. S7A). We examined if group II compounds could inhibit the activation of this mutant. Seven group II compounds (SC1, 13, 19, 23, 27, 63, and 66) led to a greater than 50% inhibition in comparison with DMSO control (Fig. S7B). Intriguingly, SC66 manifested the strongest inhibitory activity, whereas its structural analogue, SC67, showed a marginal effect. To obtain a structure–activity relationship, we further confirmed the dose-dependent inhibitory effects of these two compounds on the activation of Akt1 (e17k) (Fig. 2A). This result was consistent with their relative activity to induce Akt ubiquitination (Figs. S5C and S6C). To test if SC66 could inhibit the membrane localization of this mutant PH domain, the PH (e17k)–EGFP was expressed in HeLa cells and live cell imaging was performed. The membrane localization of PH (e17k)–EGFP was insensitive to inhibition of PI3K, as previously reported (23). However, SC66 effectively prevented its membrane localization whereas SC67 showed little inhibitory effect (Fig. 2B). When similar experiments were done with the WT PH-EGFP, both compounds effectively prevented the membrane localization (Fig. S8). Intriguingly, however, the pericentrosomal localization was more prominent in the presence of SC66. This result appears to be consistent with their relative activity in inducing Akt ubiquitination. Both SC66 and SC67 contained the pyridine moiety, and some Akt inhibitors were also shown to have this moiety (17, 18). Therefore, we also tested other pyridine-containing compounds represented in the screening library. At the comparable amount, none of these other compounds showed any inhibitory effect (Fig. 2B).

Next, we examined if Akt1 (e17k) could be also ubiquitinated by SC66. Compared with WT, Akt1 (e17k) displayed a slightly faster kinetics of ubiquitination, and the phosphorylated (S473) Akt could be also ubiquitinated in this *in vitro* reaction. It has been shown that phosphorylation at turn motif (T450) by mTorc2 complex regulates Akt maturation and stability (24, 25). However, Akt1 (e17k) showed a comparable level of phosphorylation at T450 as the WT (Fig. S9A). Nonetheless, compared with the

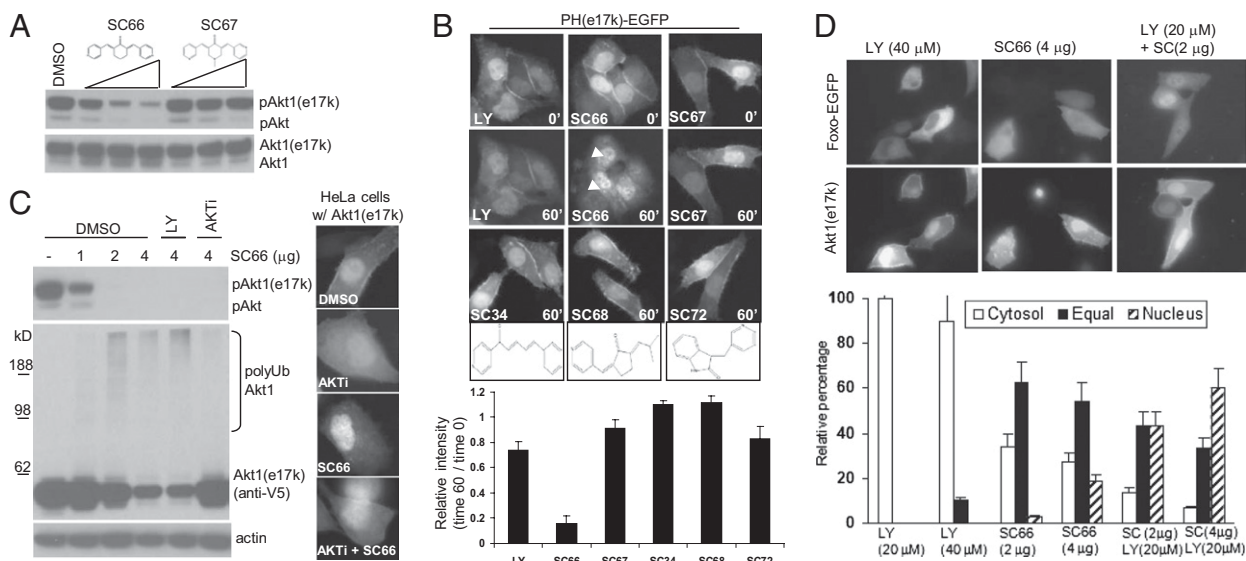


Fig. 2. SC66 functionally inhibits a cancer-relevant Akt1 (e17k) mutant. (A) HEK293 cells stably expressing Akt1 (e17k) mutant were treated with different amounts (2, 4, 8 $\mu\text{g}/\text{mL}$) of SC66 or SC67 for 1 h, followed by Western blot for phospho-Akt (S473). (B) HeLa cells expressing PH (e17k)–EGFP were treated with LY294002 (40 μM) or indicated compounds (4 $\mu\text{g}/\text{mL}$) in the presence of IGF1. The relative intensity of membrane PH (e17k)–EGFP between time 0 and 60 min was quantified. The arrows indicate the pericentrosomal accumulation of PH (e17k)–EGFP. (C) HEK293–Akt1 (e17k) cells were pretreated with LY294002 or AKTi-VIII for 30 min followed by SC66 treatment for an additional 2 h, and the cytosolic extracts were analyzed for phospho-Akt and ubiquitinated Akt1 (e17k) (Left). HeLa cells transfected with Akt1 (e17k) were treated with AKTi-VIII, SC66, or a combination of the two for 2 h. The representative immunostaining for Akt1 (e17k) is shown (Right). (D) HeLa cells cotransfected with EGFP–Foxo and Akt1 (e17k) were treated with different amounts of LY294002, SC66, or a combination of the two. The coexpressing cells were identified by immunostaining for Akt1 (e17k). The relative intensity of cytosolic versus nuclear EGFP–Foxo was determined and scored as cytosolic (>1.1), equal (1.1–0.9), or nuclear (<0.9; Right).

As a measure of cell proliferation or death, we counted the number of cells entering mitosis or undergoing apoptosis during the 14-h imaging time. In control condition, approximately 45% of cells entered mitosis, which is consistent with a doubling time of 20 to 24 h in HeLa cells. In the presence of different inhibitors of PI3K, AKTi-VIII, or SC66, this percentage was reduced to 10% to 30%, confirming the growth-inhibitory property of these chemicals. Within this time period, no dramatic cell death could be observed with all chemicals tested, including SC66 (Fig. 3B). The relative growth inhibition was correlated with the level of phosphorylated Akt in the presence of each compound (Fig. S12). When treated in HeLa cells grown in serum-rich conditions, SC66 effectively inhibited phosphorylation of both Akt and its targets. Importantly, consistent with their different mode of action in preventing Akt activation, a combined treatment of SC66 and LY294002 led to an efficient inhibition (Fig. S13A). PIP3 is required for various cellular processes, and cancer cells may activate the compensatory mechanisms when PI3K is inhibited. When treated with LY294002, the level of Akt phosphorylation reached the lowest level within the first 1 h, but was recovered in the next several hours. A similar trend was also observed with wortmannin, an irreversible PI3K inhibitor. Importantly, the kinetics and degree of recovery were almost identical between two different concentrations of wortmannin (Fig. S13B). Also, because both LY294002 and wortmannin were effective in inhibiting cell proliferation (Fig. 3B), the chemical instability alone did not explain this effect. Similarly, when HeLa cells were treated with LY294002, a prominent nuclear localization of EGFP-Foxo was observed within the first 1 h. However, after overnight treatment, most of EGFP-Foxo was localized to the cytoplasm of surviving cells (Fig. 3C). More importantly, when these HeLa cells were subsequently treated with the same amount of LY294002, only approximately 50% of cells displayed the nuclear EGFP-Foxo, indicating the activation of compensatory mechanisms. In contrast, when SC66 was administered to

these cells, an efficient inhibition of Akt activity was still observed, confirming that LY294002-resistant Akt activation could be suppressed by SC66 (Fig. 3C). If SC66 effectively suppresses the reactivation of Akt in cancer cells that had survived the inhibition of PI3K, then the combined treatment would result in an enhanced apoptosis. We examined this effect by live cell imaging of HeLa cells treated with SC66 (Movie S1), LY294002 (Movie S2), or a combination of the two (Movie S3). Surprisingly, when combined in a concentration at which neither of the two drugs alone was effective, a dramatic cancer cell death was observed (Fig. 3D, Fig. S13 C and D, and Movie S3). This synergistic cell death was not restricted to epithelial cancer cells, but was also observed in HS-Sultan cells, a lymphoma cell line (Fig. S13E).

SC66 Manifests Anticancer Activity in Vitro and in Vivo. SC66 displays a dual-inhibitory function toward Akt activity: inhibition of the initial activation by interfering with PH domain binding to PIP3 and deactivation by facilitated ubiquitination. We reasoned that, because of this dual inhibitory activity, SC66 may manifest effective anticancer activity in cancer cells with a high level of PIP3 signaling. Consistent with this prediction, compared with control, SC66 preferentially suppressed the viability of HEK cells transformed by SV40 large T antigen (HEK293T) or oncogenic Ras (HEK-Ras), both of which retained elevated Akt signaling, even in the absence of serum growth factors (Fig. S14). In addition, at a comparable concentration, SC66 resulted in a more effective inhibition of phosphorylation of Akt and its target proteins compared with LY294002 and API-2, an Akt inhibitor (29) (Fig. 4A). This biochemical result was correlated with their relative growth inhibitory effect as determined by the cell viability assay (Fig. 4B). The anticancer activity of SC66 was further supported by its potent inhibitory effects on the colony formation of HEK293T cells grown on soft agar (Fig. 4C). Finally, by using the mouse xenograft tumor model, we tested if this anticancer activity could be extended to in vivo. Seven days after the inoculation of HEK293T cells, the mice

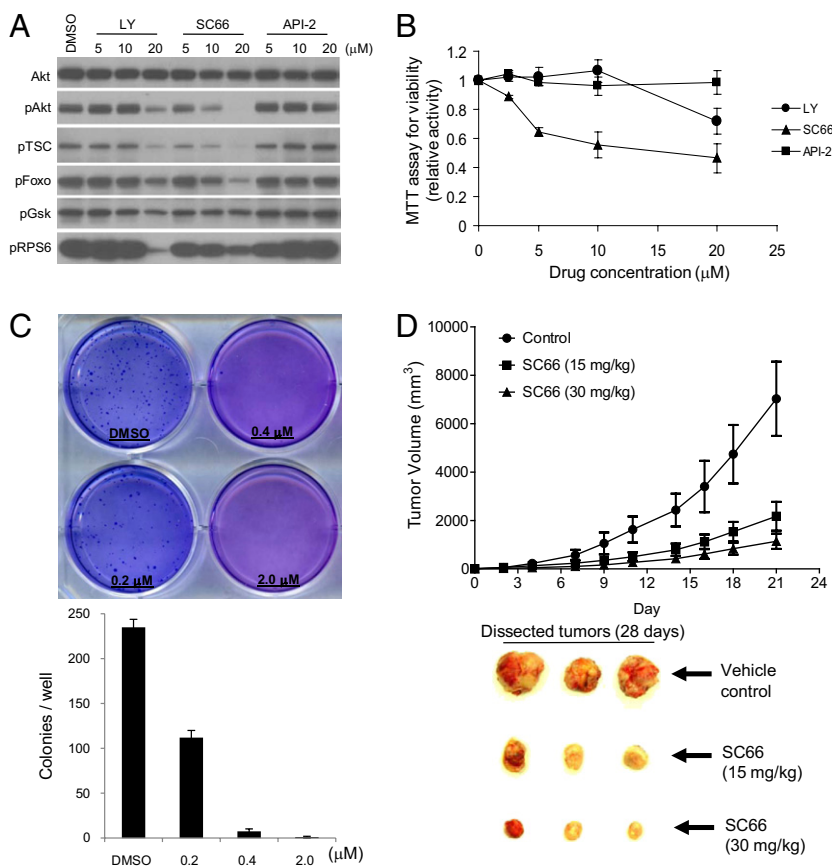


Fig. 4. SC66 manifests anticancer activity in vitro and in vivo. (A) HEK293T cells grown in serum-rich medium were treated with the indicated amounts of each compound for 1 h. The phosphorylation levels of Akt and its target proteins were examined. (B) HEK293T cells were treated with the indicated amounts of each compound for 16 h, and cell viability was determined by MTT assay. (C) Inhibitory effect of SC66 toward colony formation of HEK293T cells on soft agar. Representative image of wells following a 3-week culture in the presence of different amounts of SC66 is shown. Quantification is from three independent experiments. (D) HEK293T cells were inoculated into the nude mice, and the mice were treated with vehicle alone or two different concentrations of SC66. The growth of tumors was measured at the indicated time points. Representative images of dissected tumors after 28 d are shown. *P* values between paired groups (Student *t* test) are as follows: control vs. SC66 15 mg/kg, *P* = 0.0209; control vs. SC66 30 mg/kg, *P* = 0.0190; and SC66 15 mg/kg vs. SC66 30 mg/kg, *P* = 0.0121.

were injected with SC66 twice per week and the size of tumors was measured every 3 d for 21 d. Compared with vehicle alone, SC66 led to a significant inhibition of tumor growth, confirming the anticancer property in vivo (Fig. 4C).

Discussion

In this study, we identified a group of chemicals that inhibit Akt activation through interfering with PH domain binding to PIP3, and lead to pericentrosomal localization of Akt. Altering the spatial distribution of Akt can lead to functional perturbation by affecting substrate recognition and facilitating dephosphorylation. Elucidating the mode of action of these compounds will undoubtedly provide important new insights into the regulatory mechanisms of oncogenic PIP3/Akt signaling pathway and the development of new therapeutic strategies. We extensively characterized a pyridine-based allosteric Akt inhibitor, SC66, that directly facilitates Akt ubiquitination in vitro and in vivo. We elucidated the mechanisms of its dual inhibitory function, identified the efficacy toward a cancer-relevant and PI3K inhibitor-resistant Akt1 (e17k) mutant, and demonstrated the synergistic apoptotic activity with the PI3K inhibitor and the in vivo anticancer efficacy as a single agent. We also showed that, because of its unique dual inhibitory activity, SC66 manifested a more effective growth suppression of transformed cells compared with other inhibitors of PIP3/Akt pathway.

The phosphorylated Akt was found to be ubiquitinated in an in vitro assay. Intriguingly, the phosphorylated and ubiquitinated Akt could be hardly detectable in lysates from cells treated with SC66.

Inhibition of initial phosphorylation by preventing Akt membrane translocation may explain this finding. However, given its efficacy toward Akt dephosphorylation in HEK293T cells, which contain a high level of PIP3, also indicates other possibilities. For example, the phosphorylated Akt, when bound to SC66, might be rapidly dephosphorylated and/or the ubiquitinated Akt by SC66 might be less likely to be phosphorylated. This prediction would be consistent with its inhibitory effects toward Akt1 (e17k) mutant, which is “membrane-prone” independent of PIP3. Further studies, including the identification of cellular factors involved in SC66-mediated Akt ubiquitination, are needed to clarify these issues. As such, SC66 represents a unique chemical tool to investigate the mechanisms of ubiquitination-dependent Akt regulation in physiological and stressed conditions.

Materials and Methods

Cell Culture and Stable Cell Lines. For routine maintenance, all cell lines were cultured in medium supplemented with 10% FBS and 1% penicillin and streptomycin under 5% CO₂. HEK293, HeLa, and their derivative cell lines were maintained in DMEM. NB4 and HS-Sultan cells were cultured in RPMI medium. HeLa cell lines stably expressing PH-EGFP were described previously (30). Other stable HEK293 cell lines expressing Akt1 mutants, Akt 3, or PH-EGFP were generated by transfecting the corresponding expression plasmids and selected and maintained in the presence of G418 (Invitrogen).

Time-Lapse Live Cell Imaging for Spatial Distribution of EGFP Fusion Proteins.

HeLa cells transfected with the plasmids encoding the EGFP fusion proteins were plated into a 35-mm glass-bottom dish (MatTek) and cultured for 24 to 48 h before imaging. For PH-EGFP membrane translocation assay, cells were serum-starved in 2 mL Leibovitz L15 medium for 1 to 2 h, which was replaced with 1 mL of fresh serum-free Leibovitz L15 medium containing each compound. After 30 min incubation, IGF1 (5 ng/mL) was added and an image was taken every 5 to 10 min under a 40 \times oil objective lens. The relative fluorescent intensity at the membrane versus adjacent cytoplasm (for PH-EGFP) or cytoplasm versus nucleus (for EGFP-Foxo) was determined. Western blot and immunostaining, PIP3 ELISA, in vitro PIP3 binding, in vitro ubiquitination assay, time-lapse live cell imaging analysis for mitotic and apoptotic cells, 3-(4,5-dimethylthiazol-2-yl)-2,5-diphenyltetrazolium bromide (MTT) assay, and other related assays are described in *SI Materials and Methods*.

Mouse Xenograft Experiment. Eight-week-old female NOD/SCID mice were used in this study. Fifteen mice received an s.c. injection of 2×10^6 293T cells in the both flanks. Seven days after injection, mice were randomized into three groups ($n = 5$ mice per group) to receive vehicle (control) or SC66 15 mg/kg or 30 mg/kg i.p. SC66 dissolved in DMSO was further diluted in 0.2 mL of PBS solution containing 25% ethanol for i.p. injections. SC66 was administered twice per week (total of six times). The size of tumor was measured three times per week by using a caliper, and mice were killed on day 28 after the injection of cancer cells. The tumor volumes were calculated as length \times width² \times 0.52. Data are presented as the mean value. A Student *t* test was performed to evaluate the difference between mean values. $P < 0.05$ was considered to indicate a statistically significant difference.

ACKNOWLEDGMENTS. The authors thank all members of the H.R.L. laboratory. The screening was performed in the Institute of Chemistry and Cell Biology–Longwood Screening Facility. This study was supported by National Institutes of Health (NIH) Training Grant HL066987 (to H.J.); NIH Grants HL085100, AI076471, HL092020, and GM076084 (to H.L.); and Research Scholar grants from the American Cancer Society (to H.L. and H.C.).

- Bunney TD, Katan M (2010) Phosphoinositide signalling in cancer: Beyond PI3K and PTEN. *Nat Rev Cancer* 10:342–352.
- Engelman JA, Luo J, Cantley LC (2006) The evolution of phosphatidylinositol 3-kinases as regulators of growth and metabolism. *Nat Rev Genet* 7:606–619.
- Guertin DA, Sabatini DM (2007) Defining the role of mTOR in cancer. *Cancer Cell* 12:9–22.
- Bozulic L, Hemmings BA (2009) PI3K: Regulation of PKB activity by phosphorylation. *Curr Opin Cell Biol* 21:256–261.
- Engelman JA (2009) Targeting PI3K signalling in cancer: Opportunities, challenges and limitations. *Nat Rev Cancer* 9:550–562.
- Garcia-Echeverria C, Sellers WR (2008) Drug discovery approaches targeting the PI3K/Akt pathway in cancer. *Oncogene* 27:5511–5526.
- Knight ZA, Shokat KM (2007) Chemically targeting the PI3K family. *Biochem Soc Trans* 35:245–249.
- Zunder ER, Knight ZA, Houseman BT, Apsel B, Shokat KM (2008) Discovery of drug-resistant and drug-sensitizing mutations in the oncogenic PI3K isoform p110 alpha. *Cancer Cell* 14:180–192.
- Alaimo PJ, Knight ZA, Shokat KM (2005) Targeting the gatekeeper residue in phosphoinositide 3-kinases. *Bioorg Med Chem* 13:2825–2836.
- Apsel B, et al. (2008) Targeted polypharmacology: Discovery of dual inhibitors of tyrosine and phosphoinositide kinases. *Nat Chem Biol* 4:691–699.
- Chen J, Tang H, Hay N, Xu J, Ye RD (2010) Akt isoforms differentially regulate neutrophil functions. *Blood* 115:4237–4246.
- Luo HR, et al. (2003) Inositol pyrophosphates mediate chemotaxis in Dictyostelium via pleckstrin homology domain-PtdIns(3,4,5)P3 interactions. *Cell* 114:559–572.
- Jia Y, et al. (2007) Inositol 1,3,4,5-tetrakisphosphate negatively regulates PtdIns(3,4,5)P3 signaling in neutrophils. *Immunity* 27:453–467.
- Yang WL, et al. (2009) The E3 ligase TRAF6 regulates Akt ubiquitination and activation. *Science* 325:1134–1138.
- Suizu F, et al. (2009) The E3 ligase TTC3 facilitates ubiquitination and degradation of phosphorylated Akt. *Dev Cell* 17:800–810.
- Toker A (2009) TTC3 ubiquitination terminates Akt-ivation. *Dev Cell* 17:752–754.
- Hartnett JC, et al. (2008) Optimization of 2,3,5-trisubstituted pyridine derivatives as potent allosteric Akt1 and Akt2 inhibitors. *Bioorg Med Chem Lett* 18:2194–2197.
- Ajmani S, Agrawal A, Kulkarni SA (2010) A comprehensive structure-activity analysis of protein kinase B-alpha (Akt1) inhibitors. *J Mol Graph Model* 28:683–694.
- Fei ZL, D'Ambrosio C, Li S, Surmacz E, Baserga R (1995) Association of insulin receptor substrate 1 with simian virus 40 large T antigen. *Mol Cell Biol* 15:4232–4239.
- Kau TR, et al. (2003) A chemical genetic screen identifies inhibitors of regulated nuclear export of a Forkhead transcription factor in PTEN-deficient tumor cells. *Cancer Cell* 4:463–476.
- Badano JL, Teslovich TM, Katsanis N (2005) The centrosome in human genetic disease. *Nat Rev Genet* 6:194–205.
- Barnett SF, et al. (2005) Identification and characterization of pleckstrin-homology-domain-dependent and isoenzyme-specific Akt inhibitors. *Biochem J* 385:399–408.
- Carpton JD, et al. (2007) A transforming mutation in the pleckstrin homology domain of AKT1 in cancer. *Nature* 448:439–444.
- Ikenoue T, Inoki K, Yang Q, Zhou X, Guan KL (2008) Essential function of TORC2 in PKC and Akt turn motif phosphorylation, maturation and signalling. *EMBO J* 27:1919–1931.
- Fachinetti V, et al. (2008) The mammalian target of rapamycin complex 2 controls folding and stability of Akt and protein kinase C. *EMBO J* 27:1932–1943.
- Luo HR, et al. (2003) Akt as a mediator of cell death. *Proc Natl Acad Sci USA* 100:11712–11717.
- Manning BD, Cantley LC (2007) AKT/PKB signaling: Navigating downstream. *Cell* 129:1261–1274.
- Jo H, et al. (2010) Natural product Celestrol destabilizes tubulin heterodimer and facilitates mitotic cell death triggered by microtubule-targeting anti-cancer drugs. *PLoS ONE* 5:e10318.
- Yang L, et al. (2004) Akt/protein kinase B signaling inhibitor-2, a selective small molecule inhibitor of Akt signaling with antitumor activity in cancer cells overexpressing Akt. *Cancer Res* 64:4394–4399.
- Jo H, Jia Y, Subramanian KK, Hattori H, Luo HR (2008) Cancer cell-derived clusterin modulates the phosphatidylinositol 3'-kinase-Akt pathway through attenuation of insulin-like growth factor 1 during serum deprivation. *Mol Cell Biol* 28:4285–4299.

Supplementary Table I. Characterization of Group II compounds.

ID	Mol. Formula	M. W.	Conc. ^a μM at 8 μg/ml	Membrane translocation / localization assay ^b						PLCβ-PH Live cell 8 μg	PIP3 binding ^c Inhibition of PH domain binding to PIP3 beads	Western blot ^d Effect on pAkt level drug conc. (8 μg/ml)			EGFP-Foxo ^e Nuclear Foxo after IGF
				Akt PH High throughput		Live cell imaging			HeLa			NB4	HsSultan		
				First	Second	16 μg	8 μg	4 μg							
SC1	C ₉ N ₄ O ₄	191	42	+	+	+	+	+	-	+/-	+	+	+	++	
SC11	C ₁₈ H ₁₄ N ₂ O ₅	338	24	+	+	+	+	+	-	+	+	+	+	++	
SC13	C ₂₁ H ₁₇ N ₄ O ₃ SBr	456	18	+	+	+	+	+	-	++	+	n.d.	n.d.	++++	
SC19	C ₁₄ N ₂ OCl ₂	282	28	+	+	+	+	+	+/-	+++	+	+	+	++	
SC23	C ₁₈ H ₁₄ N ₄ O ₃ S	326	25	+	+	+	+	+	-	+++	+	+	-	++++	
SC27	C ₁₉ H ₇ NOS	189	42	+	+	+	+	+	-	++	+	+	-	++++	
SC49	C ₁₈ H ₁₁ N ₃ O ₆	365	22	+	+	+	+	+	-	+	+	+	+	+++	
SC63	C ₁₃ H ₁₂ N ₂ O ₂ S ₂	292	27	+	+	+	+	+	-	++	+	+	+	+	
SC66	C ₁₈ H ₁₈ N ₂ O	276	29	+	+	+	+	+	-	+++	+	+	+	++	
SC67	C ₁₈ H ₁₇ N ₃ O	291	27	+	+	+	+	+/-	-	++	+	+	+	++	
SC86	C ₁₈ H ₁₆ N ₄ O ₂ S ₂	384	21	+	+	+	+	+	-	+	+	n.d.	n.d.	+	
E26	C ₁₁ H ₈ NO ₃	203	39	+	+	+	+	+	-	++	+	+	+	+	

Supporting Information

Jo et al. 10.1073/pnas.1019062108

SI Discussion

Deactivation of PIP3/Akt signaling pathway suppresses the growth of tumors and the resistance of cancer cells to chemotherapeutic drugs (1–4). The signaling pathways for PIP3 production and the mechanisms of PIP3-mediated Akt activation are well established and broadly applicable to different cell types. However, how the activated Akt is deactivated in specific cellular contexts remains to be elucidated. Facilitating the deactivation of Akt would enhance the efficacy of various inhibitors of PI3K, which prevent only the activation step. Inhibiting the kinase activity of Akt will be an obvious choice. However, as elegantly demonstrated in a recent study (5), paradoxically, chemicals targeting the Akt kinase domain were shown to lead to the “inhibitor-induced Akt activation,” raising concerns for the long-term clinical utility of such inhibitors (5).

Akt is known to undergo dynamic conformational changes. Controlling the structural integrity of Akt appears to serve as another regulatory mechanism. For example, it has been reported that mTorc2, apart from its activity as an S473 kinase, plays important roles in maintaining the structural integrity and maturation of Akt by phosphorylating at T450 in turn motif (6, 7). Lack of phosphorylation at this site, as a result of genetic ablation of mTorc2 components, results in the structural instability of Akt, leading to an increased susceptibility to proteasome-dependent degradation. We showed that, compared with WT, Akt1 (e17k) was unstable upon inhibition of HSP90. However, this instability did not appear to be caused by the lack of phosphorylation at T450. A recent study reported an enhanced ubiquitination of Akt1 (e17k) mutant by TRAF6 E3 ubiquitin ligase, which facilitates its membrane localization and activation (8). We also found a faster kinetics of SC66-induced ubiquitination of this mutant.

How this mutation in PH domain leads to an enhanced Akt ubiquitination is not clear. Further studies, including the identification of cellular factors involved in SC66-induced Akt ubiquitination, are needed. Ectopic expression of TRAF6 or CHIP E3 ubiquitin ligases known to be involved in Akt ubiquitination (8, 9), failed to affect the SC66-induced Akt ubiquitination. Also, as SC66 inhibits Akt phosphorylation, the drug-bound Akt is unlikely to be directly ubiquitinated by TTC E3 ubiquitin ligase, which was shown to specifically bind to and ubiquitinate the phosphorylated Akt (10).

A wide variety of PI3K inhibitors have been developed and are continuously being identified. One caveat of suppressing PIP3 signaling in cancer cells by PI3K inhibitor alone is the activation of compensatory mechanisms, as demonstrated in HeLa cells treated with LY294002 or wortmannin. Likewise, targeting the Akt activity alone can be compensated by other AGC family member kinases. Considering the heterogeneity and various genetic lesions of cancers, the effective termination of Akt signaling requires a multifaceted strategy that prevents the membrane translocation and facilitates its deactivation. The dual-function allosteric inhibitor elucidated in this study exemplifies one such new strategy.

SI Materials and Methods

Reagents and Antibodies. Plasmids encoding human Akt1 were initially obtained from Dana–Farber/Harvard Cancer Center DNA Resource Core and subcloned into the pcDNA3.1/V5-His-TOPO vector. The site-directed mutagenesis was done with the QuikChange mutagenesis kit (Stratagene). EGFP-Foxo1 was obtained from Addgene. All Akt- and phosphorylation-specific antibodies were purchased from Cell Signaling Technology; V5

antibody was from Invitrogen; ubiquitin antibody (sc-9133) was from Santa Cruz Biotechnology. All other reagents, including the HRP-conjugated secondary antibodies, for Western blot were from GE Healthcare. LY294002, Akt inhibitors, rapamycin, and wortmannin were purchased from EMD Biosciences; PI-103, PIP3-coated beads, and PIP3 ELISA kit were from Echelon.

Western Blot and Immunostaining. Preparation of cell lysates, SDS/PAGE, and Western blot, and other standard molecular biological techniques, were essentially the same as described previously (11). For immunostaining of Akt1 (1:2,000 for V5 antibody) and phospho-Akt (1:200 for pS473), cells were fixed in 3% paraformaldehyde, and followed the same procedure as previously described (12).

PIP3 ELISA and in Vitro PIP3 Binding Assay with Purified PH-EGFP Protein. The serum-starved HeLa cells (1×10^7) were pre-treated with LY294002 (20 μ M) or group II chemicals (4 μ g/mL) for 30 min, then stimulated with IGF1 (5 ng/mL) for 20 min. Extraction of PIP3 by sequential centrifugation in methanol:chloroform:HCl buffer and measurement of the extracted PIP3 was done using the PIP3 Mass ELISA Kit (K-2500s; Echelon), according to the instructions. For purification of PH-EGFP protein, HEK cells (1×10^8) stably expressing PH-EGFP tagged with the C-terminal V5/His were suspended in PBS solution containing 0.3% CHAPS, 20 mM imidazole, and protease inhibitor mixtures. The cell suspension was frozen on dry ice for 30 min and thawed at room temperature. The lysates were cleared by centrifugation and loaded on the column packed with Ni-NTA beads (Qiagen). After washing three times in PBS solution containing 0.3% CHAPS and 50 mM imidazole, the bound fraction was eluted with 100 mM imidazole. The eluted protein was concentrated in the binding buffer (10 mM Hepes, pH 7.4, 0.25% Nonidet P-40, 150 mM NaCl, 0.5 mM β -mercaptoethanol) by centrifugation (Amicon Ultra 10K cutoff filter; Millipore). The purified PH-EGFP protein (800 ng/mL) was preincubated with group II compounds (1 μ g/mL) for 20 min on ice, and incubated with 20 μ L of PIP3-coated beads (Echelon) for overnight at 4 $^{\circ}$ C. After washing the beads three times with binding buffer at room temperature, the amount of bead-bound PH-EGFP protein was determined by Western blot.

Proteasome, Deconjugation, and in Vitro Ubiquitination Assay Using Cell Lysates. HEK293 cells (1×10^6) were treated with compounds (4 μ g/mL) for 1 h. After washing with PBS solution, the cell pellet was lysed on ice for 15 min in 200 μ L lysis buffer (20 mM Tris-HCl, pH 7.5, 150 mM NaCl, 1 mM EDTA, 1 mM EGTA, 1 mM β -glycerophosphate, 1% Triton X-100). After clearing cell debris by centrifugation at 4 $^{\circ}$ C, the extract (50 μ L) was subjected to proteasomal activity using Proteasome-Glo Chymotrypsin-Like Assay (G8621; Promega). The same extract was also assayed for deconjugation activity by using DUB-Glo Protease Assay (G6260; Promega). For in vitro ubiquitination assay, HEK293 expressing Akt1 tagged with V5/HIS were lysed in a buffer containing 50 mM Hepes, pH 7.4, 0.2% Nonidet P-40, 0.5 mM β -mercaptoethanol, and protease inhibitor mixtures. The lysates were frozen on dry ice for 30 min and thawed at room temperature. After centrifugation, the extract was subjected to in vitro ubiquitination reaction. Typically, 100 to 200 μ g of total proteins were mixed with 1 μ g of chemicals on ice for 10 min, and supplemented with MG132 (5 μ M), ubiquitin aldehyde (4 μ M), and ATP (5 mM) in 50 μ L of ubiquitin conjugation reaction

buffer (Boston Biochem), and incubated for 1 h followed by Western blot.

Time-Lapse Live Cell Imaging Analysis for Mitotic and Apoptotic Cells. HeLa cells growing exponentially (or approximately 65%–70% confluence) in 35 mm dish were replaced with 2 mL of Leibovitz L15 medium supplemented with 10% FBS and cultured for 2 h, and then compounds were added. The time-lapse movie was taken every 15 min for 14 to 16 h. Each movie frame in the 14-h time period was analyzed for mitotic or apoptotic cells as previously described (12). The mitotic cells were identified as they underwent morphological changes from flat to round shape and cell division in later frames, and the apoptotic cells were identified as their membrane collapsed and lost adhesion to the plate.

1. Fan QW, et al. (2006) A dual PI3 kinase/mTOR inhibitor reveals emergent efficacy in glioma. *Cancer Cell* 9:341–349.
2. Knight ZA, et al. (2006) A pharmacological map of the PI3-K family defines a role for p110alpha in insulin signaling. *Cell* 125:733–747.
3. Pomel V, et al. (2006) Furan-2-ylmethylene thiazolidinediones as novel, potent, and selective inhibitors of phosphoinositide 3-kinase gamma. *J Med Chem* 49:3857–3871.
4. Luo HR, et al. (2003) Akt as a mediator of cell death. *Proc Natl Acad Sci USA* 100: 11712–11717.
5. Okuzumi T, et al. (2009) Inhibitor hijacking of Akt activation. *Nat Chem Biol* 5: 484–493.
6. Ikenoue T, Inoki K, Yang Q, Zhou X, Guan KL (2008) Essential function of TORC2 in PKC and Akt turn motif phosphorylation, maturation and signalling. *EMBO J* 27: 1919–1931.
7. Facchinetti V, et al. (2008) The mammalian target of rapamycin complex 2 controls folding and stability of Akt and protein kinase C. *EMBO J* 27:1932–1943.
8. Yang WL, et al. (2009) The E3 ligase TRAF6 regulates Akt ubiquitination and activation. *Science* 325:1134–1138.
9. Dickey CA, et al. (2008) Akt and CHIP coregulate tau degradation through coordinated interactions. *Proc Natl Acad Sci USA* 105:3622–3627.
10. Suizu F, et al. (2009) The E3 ligase TTC3 facilitates ubiquitination and degradation of phosphorylated Akt. *Dev Cell* 17:800–810.
11. Jo H, Jia Y, Subramanian KK, Hattori H, Luo HR (2008) Cancer cell-derived clusterin modulates the phosphatidylinositol 3'-kinase-Akt pathway through attenuation of insulin-like growth factor 1 during serum deprivation. *Mol Cell Biol* 28:4285–4299.
12. Jo H, et al. (2010) Natural product Celastrol destabilizes tubulin heterodimer and facilitates mitotic cell death triggered by microtubule-targeting anti-cancer drugs. *PLoS ONE* 5:e10318.

MTT Assay. HEK293T cells (2.5×10^5) were plated in a 24-well plate in 500 μ L of phenol red-free medium supplemented with 10% FBS. The next day, different amounts of each compound were added and cultured overnight (16–20 h), and 50 μ L of MTT solution (5 mg/mL) were added to each well and incubated for 2 h. After directly adding 500 μ L of isopropanol with 0.1 M HCl to each well to dissolve the crystals, the absorbance was measured at a wavelength of 570 nm.

Soft-Agar Colony Formation Assay. A 0.6% agar gel with 10% FBS in DMEM was prepared and added to a six-well culture dish as a base agar. HEK293T cells (3,000 per well) were plated in 0.3% agar gel with 10% FBS in DMEM supplemented with different concentrations of SC66 on top of the base agar and allowed to grow for 3 wk. Colonies were stained with Crystal violet dye. The results represent the averages from three independent experiments.

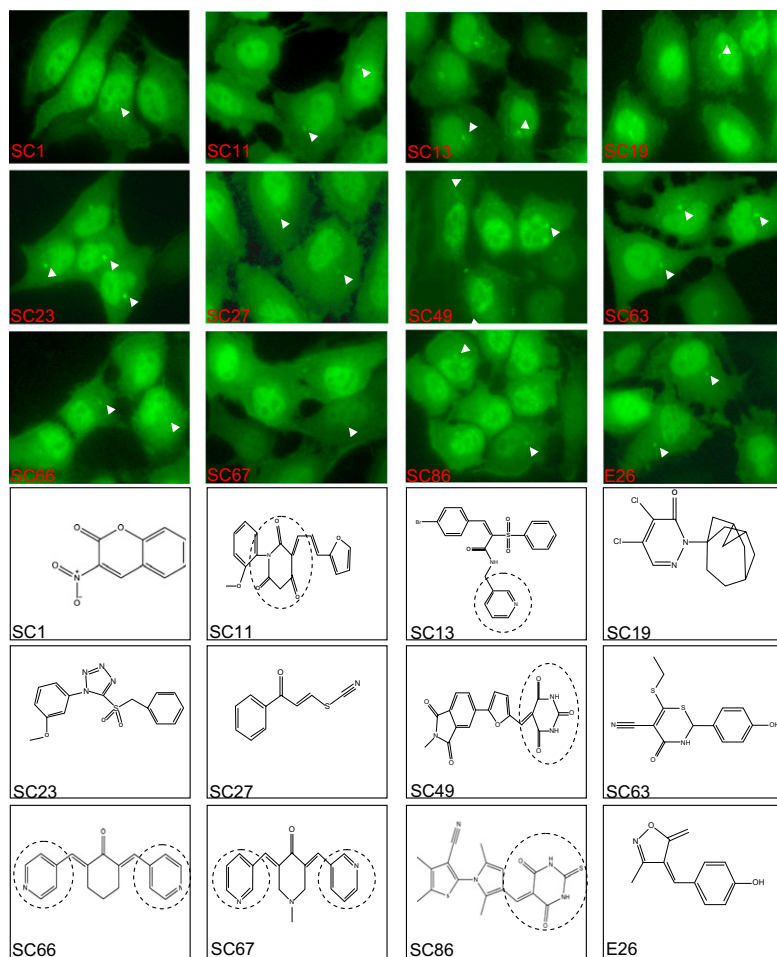


Fig. S1. Representative pictures of live imaging of HeLa-EGFP cells treated with group II compounds (chemical structures, *Bottom*). Arrows indicate the pericentrosomal region. Dotted circles indicate the barbiturate-derivative and pyridine moiety.

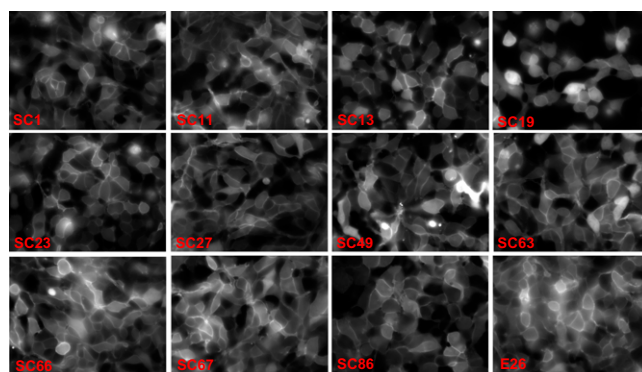


Fig. S2. The effect of group II compounds (8 $\mu\text{g}/\text{mL}$) on the PtdIns(4,5)P₂-mediated membrane localization of EGFP-PLC- δ 1-PH domain.

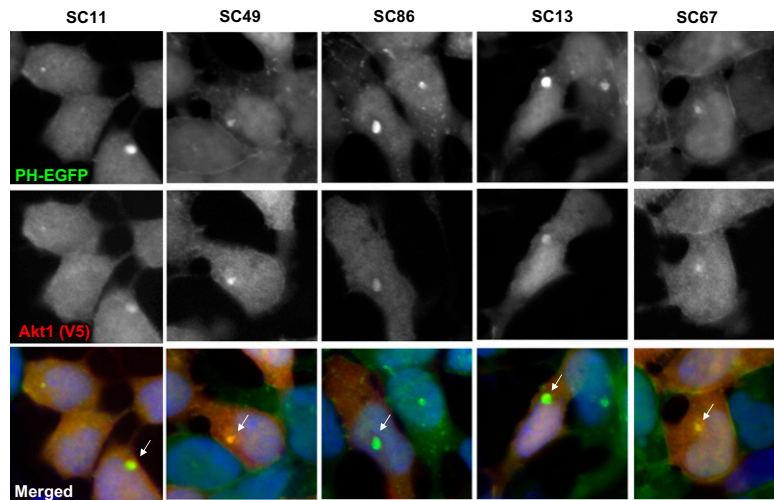


Fig. S3. HEK293 cells stably expressing PH-EGFP were transfected with the C-terminal V5/His-tagged Akt1. Following treatment with the indicated group II compounds (4 $\mu\text{g}/\text{mL}$) for 1 h, the fixed cells were stained for Akt1. Colocalization with PH-EGFP in pericentrosomal region is indicated by arrows.

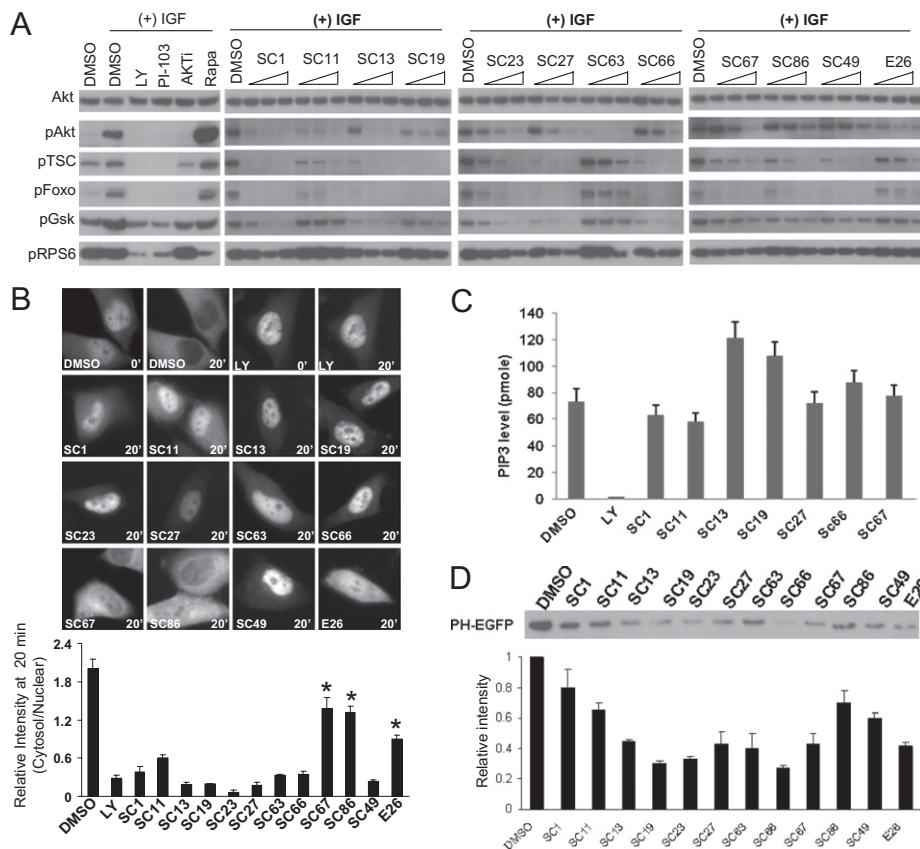


Fig. S4. (A) Serum-starved HeLa cells were treated with the known inhibitors of PI3K (LY294002 and PI-103), Akt (AKTi-VIII), mTorc1 (rapamycin), or three different concentrations (2, 4, or 8 $\mu\text{g}/\text{mL}$) of group II compounds for 30 min and stimulated with IGF (5 ng/mL) for an additional 30 min. The cell lysates were analyzed for the level of Akt phosphorylation at S473. The same blot was also probed for phosphorylation of the indicated target proteins. (B) HeLa cells transfected with EGFP-Foxo were serum-starved and treated with group II compounds for 30 min (4 $\mu\text{g}/\text{mL}$). Following addition of IGF1 (5 ng/mL), a live cell image was taken every 5 min. Representative image at 20 min IGF1 stimulation in the presence of each compound is shown. The intensity of cytoplasm and nuclear EGFP-Foxo was quantified, and the relative ratio is presented (Bottom; $*P < 0.05$, Student *t* test). (C) Serum-starved HeLa cells were treated with DMSO, LY294002 (20 mM), or the indicated group II compounds (4 $\mu\text{g}/\text{mL}$) for 30 min, followed by IGF1 (5 ng/mL) stimulation for 20 min. The amount of cellular PIP3 was measured by ELISA and calculated in reference to the standard PIP3 lipid. (D) The purified PH-EGFP protein (800 ng/mL) was preincubated with group II compounds (1 $\mu\text{g}/\text{mL}$) for 20 min on ice followed by incubation with the PIP3-coated beads overnight in a cold room. After washing, the bead-bound fraction was resolved on SDS/PAGE and blotted with the V5 antibody. Representative blot is shown, and the quantification is the average of three independent experiments.

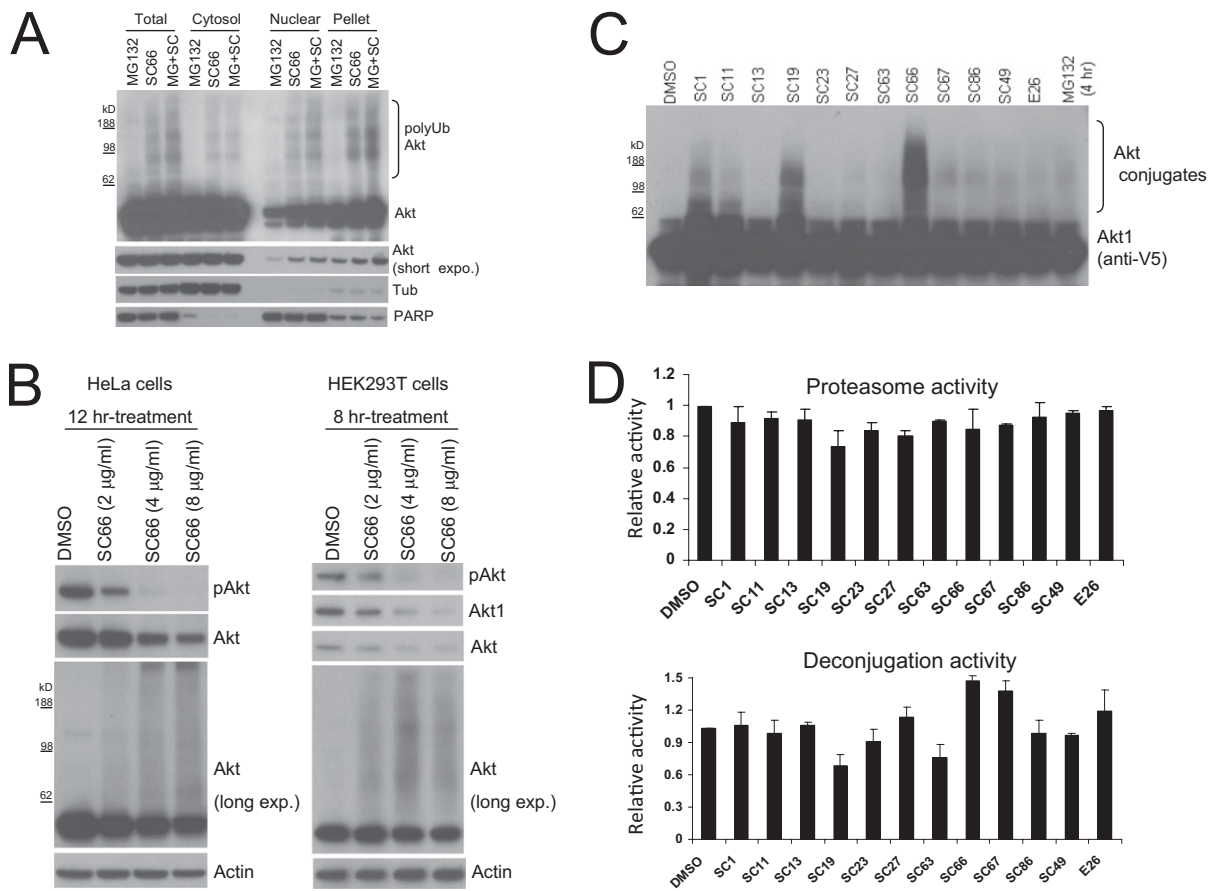


Fig. 55. (A) HeLa cells were pretreated with MG132 (10 μ g/mL) for 2 h before addition of SC66 (4 μ g/mL). Following an additional 2-h incubation, the total cell extract, cytosolic, nuclear, or pellet (insoluble) fraction were analyzed for Akt. The same fractions were simultaneously blotted for other cellular proteins: β -tubulin for cytosolic and PARP for nuclear fractions, respectively. (B) HeLa or HEK293T cells were treated with different amounts of SC66 for the indicated time points and the levels of pAkt, Akt, and actin were analyzed. (C) HEK293 cells stably expressing Akt1, HEK293-Akt1, were treated with group II compounds (4 μ g/mL) for 1 h or MG132 (10 μ g/mL) for 4 h, and the cell lysates were analyzed for Akt1 by Western blot with a monoclonal V5 antibody. (D) Proteasomal and deconjugation activity from the cytosolic cell lysates were measured. Relative activity in reference to DMSO-treated cells is presented.

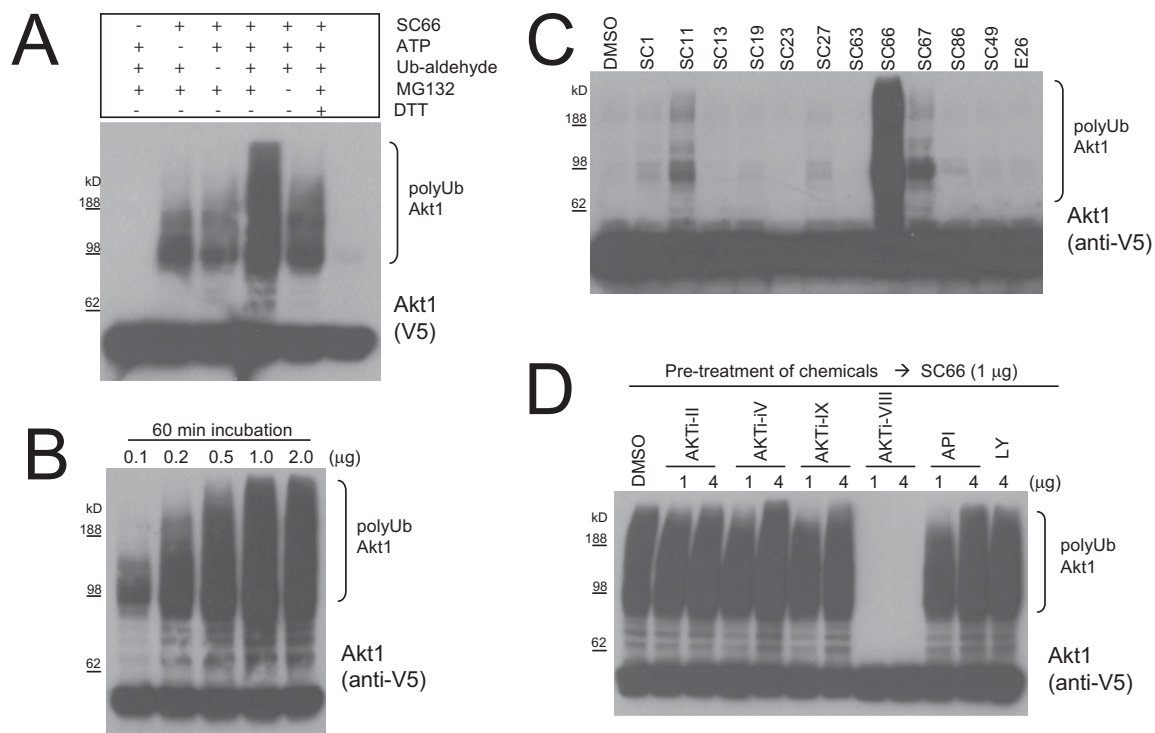


Fig. 56. (A) SC66-induced in vitro ubiquitination assay for Akt. HEK293-Akt1 cell lysates were incubated with the indicated combinations of ATP, ubiquitin aldehyde, MG132, DTT, and SC66 for 1 h. The absence of ubiquitin aldehyde, which inhibits deubiquitination, most significantly affected the Akt ubiquitination. The ubiquitinated Akt detected in the absence of additional ATP could be a result of residual ATP and preformed E1- and E2-ubiquitin complex present in the cell extract. In the presence of DTT, which disrupts the thioester bond between E1- and E2-ubiquitin that is required for the subsequent ubiquitination by E3 ligases, the SC66-induced Akt ubiquitination was almost completely abolished. (B) SC66 dose-dependent in vitro ubiquitination of Akt. (C) The effect of group II compounds on the in vitro ubiquitination of Akt1. (D) The effects of AKTi-VIII and other chemicals known to inhibit Akt pathway on in vitro ubiquitination of Akt1 by SC66. The indicated amounts of chemicals were pre- or simultaneously incubated with SC66, followed by in vitro ubiquitination reaction.

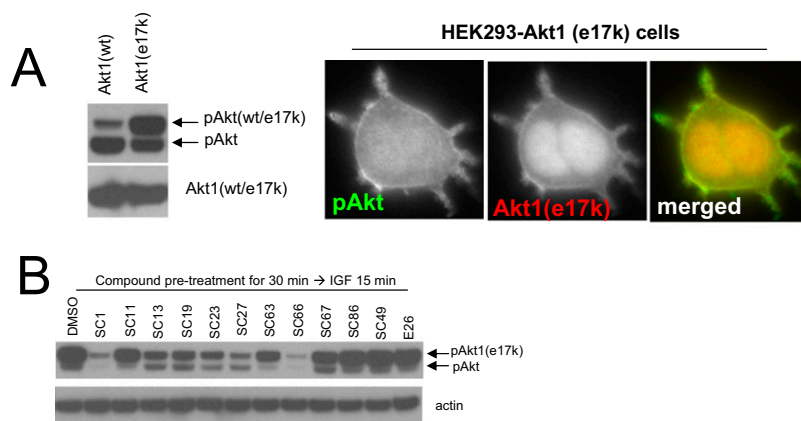


Fig. 57. (A) Level of phospho-Akt and cellular localization of Akt1 (e17k). (B) Inhibitory effects of group II compounds (8 μg/mL) on the phosphorylation of Akt1 (e17k).

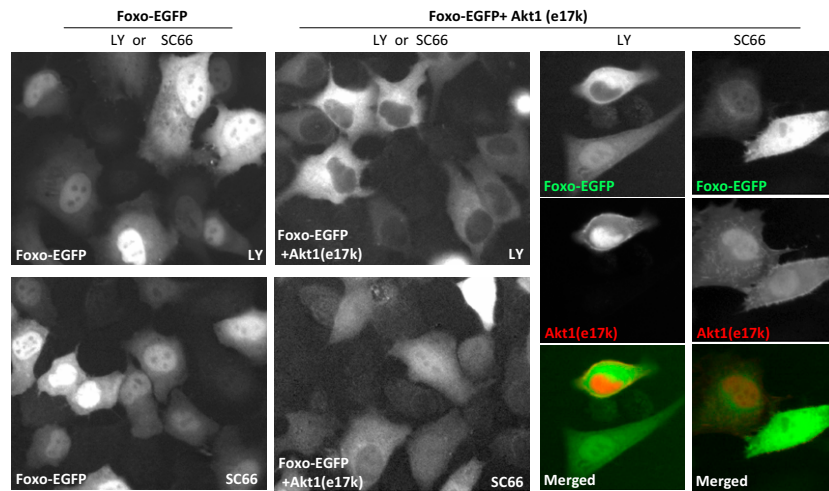


Fig. S10. Effect of LY294002 (40 μ M) or SC66 (4 μ g/mL) on the cellular localization of EGFP-Foxo in HeLa cells expressing Akt1 (e17k) mutant. HeLa cells were transfected with EGFP-Foxo alone or cotransfected with Akt1 (e17k) and treated with the chemicals for 1 h. Representative immunostaining shows coexpression of EGFP-Foxo and Akt1 (e17k).

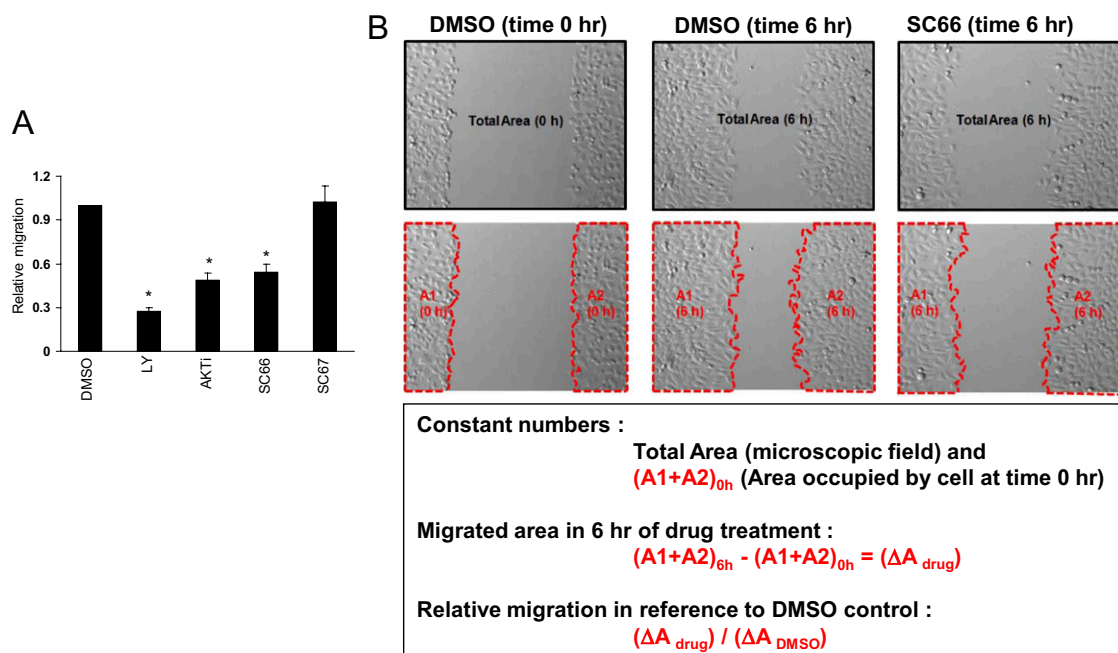


Fig. S11. (A) Quantification of cell migration in Fig. 3A. The relative migration area compared with DMSO control was presented. * $P < 0.05$ by Student t-test. (B) A schematic presentation of the quantification of HeLa cell migration in Fig. 3A.

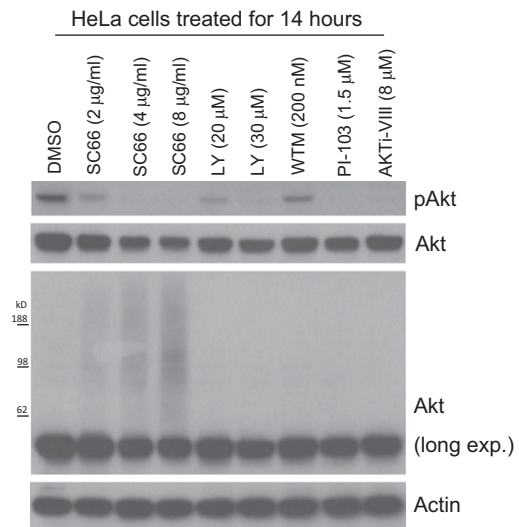


Fig. S12. Effects of long-term treatment with chemicals, as in Fig. 3B, on the levels of phosphorylated Akt in HeLa cells.

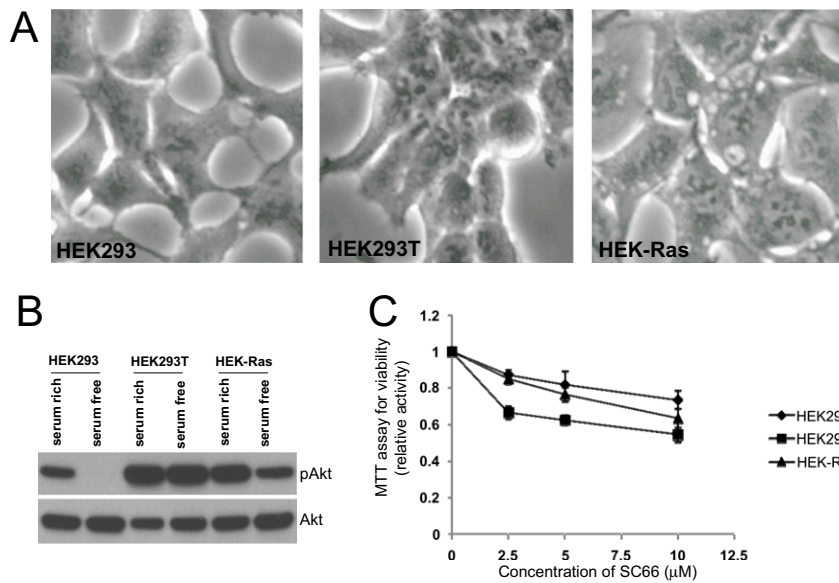
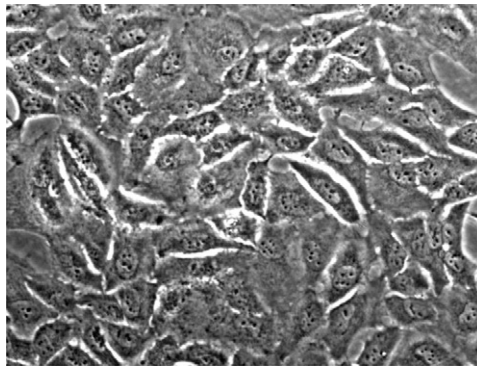
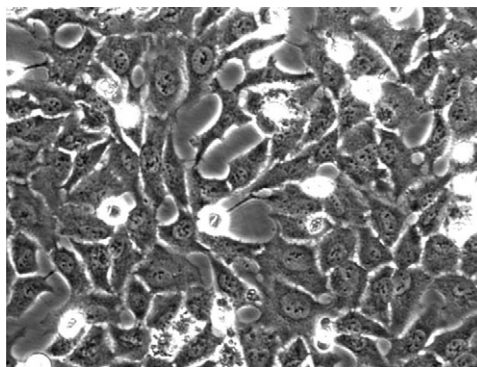


Fig. S14. (A) Morphology of the parental HEK293 cells and cells transformed by SV40 large T antigen (HEK293T) or H-Ras oncogene (HEK-Ras). (B) The level of phosphorylated Akt in cells grown in serum-rich or serum-free (for 1 h starvation) medium. (C) Differential growth-suppressive effects of SC66 on parental HEK cells and transformed cells. The relative viability was determined after 24 h treatment with SC66.



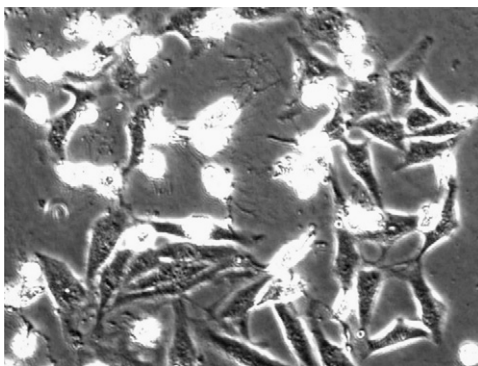
Movie S1. Live cell imaging of HeLa cells treated with SC66 (2 μg/mL). Frames were taken every 15 min for 14 h.

[Movie S1](#)



Movie S2. Live cell imaging of HeLa cells treated with LY294002 (20 μM). Frames were taken every 15 min for 14 h.

[Movie S2](#)



Movie S3. Live cell imaging of HeLa cells treated with SC66 and LY294002. Frame were taken every 15 min for 14 h.

[Movie S3](#)

Dataset S1. Characterization of group II compounds

[Dataset S1 \(XLS\)](#)

^a8 $\mu\text{g}/\text{mL}$ is the equivalent to 1 \times concentration of the initial high-throughput screening.

^bPlus signs indicate inhibition of membrane translocation greater than 50% of control.

^cNumber of plus signs represents the relative inhibitory activity compared with DMSO control.

^dPlus signs indicate inhibition of Akt phosphorylation (s473) greater than 50% of control.

^eNumber of plus signs represents the relative intensity of nuclear EGFP-Foxo over cytoplasm.